International Journal of Biological Macromolecules 95 (2017) 24–31

Contents lists available at ScienceDirect

International Journal of Biological Macromolecules

journal homepage: www.elsevier.com/locate/ijbiomac

Reversibility of strain stiffening in silk fibroin gels

Zeynep Oztoprak, Oguz Okay*

Istanbul Technical University, Department of Chemistry, 34469 Maslak, Istanbul, Turkey

ARTICLE INFO

Article history:
Received 26 July 2016
Received in revised form 19 October 2016
Accepted 10 November 2016
Available online 12 November 2016

Keywords:
Silk fibroin
Hydrogels
Strain stiffening

ABSTRACT

We investigate the linear and nonlinear viscoelastic properties as well as the reversibility of strain-stiffening behavior of silk fibroin gels. The gels are prepared from 4.2 w/v% fibroin solution in the presence of butanediol diglycidyl ether and *N,N,N′,N′*-tetramethylethylenediamine (TEMED) as a cross-linker and catalyst, respectively. By changing the concentration of TEMED in the gelation system, fibroin gels exhibiting a storage modulus G' between 10^{-1}–10^{5} Pa and a loss factor *tan* δ between 10^{-2} and 10° could be obtained. We observe a strong stiffening (up to 900%) in fibroin gels with increasing strain above 10% deformation, but reversibly if the strain is removed, the gel recovers its initial viscoelastic properties. The strain induced formation of transient intermolecular domains acting as reversible cross-links are responsible for the stiffening behavior of fibroin gels. These additional cross-links formed in the hardened fibroin gels have a temporary nature with lifetimes of the order of seconds. The nonlinear behavior of fibroin gels can be reproduced by a wormlike chain model taking into account the entropic elasticity of fibroin molecules and the strain induced increase in the cross-link density of fibroin gels.

1. Introduction

Silk fibroin gels and scaffolds attract significant interest for biomedical and biotechnological applications due to the extraordinary mechanical properties, biocompatibility, and controlled degradability [1–3]. Sol-gel transition in aqueous silk fibroin solutions mainly occurs by self-assembly of fibroin molecules via hydrophobic interactions to form intermolecular β-sheet crystallites acting as physical cross-links [4,5]. Self-assembly of silk fibroin from random coil to β-sheet structure and following gelation can be induced by pH [6–14], temperature [6,7], fibroin concentration [5,7,9], cations [13–17], diepoxide cross-linkers [18,19], vortexing [20], and electrical field [21–23]. In silk fibroin gels, fibroin molecules are interconnected by physical but essentially irreversible cross-link zones consisting of β-sheet nanostructures.

Strain induced stiffening accompanied by an increase in the storage modulus of fibroin gels has also been reported in a few studies [18,24]. Strain-stiffening is in fact an inherent property of many biological gels consisting of semiflexible or rigid filaments [25–29]. The strain-stiffening behavior enables the resistance of biological gels against large deformations and thus, it can be considered as a nature's defense mechanism against the external forces to protect the tissue integrity. For instance, a significant stiffening at very small deformations (~10%) was reported for gels formed from semiflexible polymers with persistence lengths of a few micrometers such as fibrin [29], and actin filaments (F-actin) [27], which are the major components of blood clots and cytoskeleton, respectively. The gels derived from collagen, the most abundant extracellular protein, exhibit slight softening at small strains following by a stiffening regime at strains γ_o above 0.2 whereas the network ruptures beyond $\gamma_o = 0.75$ [30]. The stiffening behavior of collagen network was attributed to the deformation induced increase in the cross-link density via network rearrangement and to the nonlinear stretching of the molecules [30]. A strain-stiffening induced by decreasing the contour length of DNA strands between cross-links was also reported in DNA gels at short experimental time scales while they soften at longer times [31].

A shear thickening followed by shear-thinning behavior was observed in aqueous fibroin solutions at or above 4.2 wt.% fibroin [9,10,15], similar to the behavior of aqueous solutions of associative polymers such as hydrophobically modified hydrophilic polymers [32,33]. It was also shown that the aqueous solutions of fibroin at concentrations of above 25 wt.% exhibit strain induced crystallization into β-sheet structure at shear rates above 2 s^{-1} [11]. We recently observed that the mechanical response of fibroin gels produced via diepoxide-triggered conformational transition of fibroin from random coil to β-sheet structure is highly nonlinear with strain-stiffening behavior (up to 700%) arising from the alignment of the crystallizable amino acid segments [18]. Moreover, the so-called e-gels produced by utilizing electrochemistry to convert the

* Corresponding author.
E-mail address: okayo@itu.edu.tr (O. Okay).

http://dx.doi.org/10.1016/j.ijbiomac.2016.11.034
0141-8130/

fibroin solution into a fibroin gel with a storage modulus G' of ~10 Pa and a loss factor *tan* δ of ~0.1 exhibit stiffening behavior at strain amplitudes γ_o above 5 and an extraordinary large yield strain [22,23]. Interestingly, e-gels exhibit reversible shear stiffening at low shear amplitudes followed by irreversible stiffening at high shear amplitudes. The results thus reveal dynamic nature of electric field induced physical cross-links between silk fibroin molecules below a critical shear stress.

In the present work, we investigate the linear and nonlinear viscoelastic properties as well as the reversibility of strain-stiffening behavior of silk fibroin gels exhibiting a storage modulus G' between 10^{-1}–10^5 Pa and a loss factor *tan* δ between 10^{-2} and 10°. We use a synthetic strategy developed recently by our group to produce fibroin gels with tunable properties [18,19]. Fibroin gels are prepared from 4.2 w/v% fibroin solution in the presence of butanediol diglycidyl ether (BDDE) cross-linker. BDDE cross-links between fibroin molecules triggers the conformational transition from random coil to β-sheet structure and hence fibroin gelation in a short period of time. By changing the concentration of *N,N,N',N'*-tetramethylethylenediamine (TEMED) catalyst in the gelation system, fibroin gels with a wide range of viscoelastic properties could be obtained. Such gels are a good candidate to understand the nonlinear viscoelastic response of interconnected fibroin molecules depending on the characteristics of fibroin gels. As will be seen below, we observe a strong stiffening in fibroin gels with increasing strain above 0.1, but reversibly if the strain is removed, the gel recovers its initial viscoelastic properties. We also show that the strain induced formation of transient intermolecular domains acting as cross-links are responsible for the stiffening behavior of fibroin gels. These additional cross-links formed in hardened fibroin gels have a temporary nature with lifetimes of the order of seconds. The nonlinear behavior of fibroin gels can be reproduced by a wormlike chain model taking into account the entropic elasticity of fibroin molecules and the strain induced increase in the cross-link density of fibroin gels.

2. Experimental

2.1. Materials

Butanediol diglycidyl ether (BDDE, Sigma-Aldrich), N,N,N',N'-tetramethylethylenediamine (TEMED, Merck), Na_2CO_3, and LiBr were used as received. Bombyx mori cocoons were purchased from Koza Birlik (Agriculture Sales Cooperative for Silk Cocoon, Bursa, Turkey). To separate silk fibroin from cocoons in the form of an aqueous solution, the method described by Kim et al. was utilized [6]. The sericin proteins were first removed from cocoons by boiling for 1 h in aqueous solution of 0.02 M Na_2CO_3. The remaining silk fibroin was then thoroughly washed three times with distilled water at 70 °C for 20 min each. The silk fibroin was dissolved in aqueous 9.3 M LiBr at 60 °C for 4 h, then dialyzed using dialysis tubing (10,000 MWCO, Snake Skin, Pierce) for 3 days against water that was changed three times a day. After centrifugation, the final concentration of silk fibroin in aqueous solution was about 5 w/w%, which was determined by weighing the remaining solid after drying.

2.2. Fibroin gelation

Silk fibroin gels were made by mixing aqueous silk fibroin solutions with BDDE cross-linker and TEMED catalyst and then placing the solution between the parallel plate of the Rheometer system to conduct the gelation reactions at 50 °C. Typically, 5 mL of 5 w/v% silk fibroin solution were mixed with 0.50 mL BDDE and an aqueous solution of TEMED to obtain a final volume of 6 mL. The concentrations of silk fibroin and BDDE were fixed at 4.2 w/v% and 20 mmol epoxide groups/g silk fibroin, respectively, while the amount of TEMED was varied between 0 and 0.7 v/v%.

2.3. Rheological experiments

Gelation reactions and the viscoelastic properties of the resulting fibroin gels were investigated using a Bohlin Gemini 150 Rheometer system (Malvern Instruments, UK) equipped with a Peltier device for temperature control. The fibroin solutions containing BDDE cross-linker and TEMED catalyst were placed between the parallel plate of the instrument. The upper plate (diameter 40 mm) of the rheometer was set at a distance of 500 μm before the onset of the reactions. During the rheological measurements, a solvent trap was used and the upper plate was covered with a thin layer of low-viscosity silicone oil to prevent evaporation of water. Gelation reactions were carried out at a frequency of $\omega = 6.3$ rad s^{-1} and a deformation amplitude $\gamma_o = 0.01$ to ensure that the oscillatory deformation is within the linear regime. Then, frequency-sweep tests at $\gamma_o = 0.01$ were carried out at 25 °C over the frequency range 6×10^{-3} to 6.3×10^{-2} rad.s^{-1}. The gels were also subjected to stress-relaxation experiments at 25 °C. A shear deformation of predetermined strain amplitude γ_o was applied to the gel samples and the resulting stress $\sigma\ (t, \gamma_o)$ was monitored as a function of time. Here, we report the relaxation modulus $G\ (t, \gamma_o)$ as functions of the relaxation time t and strain amplitude γ_o. The experiments were conducted with increasing strain amplitudes γ_o from 0.01 to 1. For each fibroin gel, stress-relaxation experiments at various γ_o were conducted starting from a value of the relaxation modulus deviating less than 10% from the modulus measured at $\gamma_o = 0.01$.

We have to note that the software of the rheometer assumes a linear rheological response of the gels within each cycle of the oscillatory deformation tests. To characterize the non-linear properties of fibroin gels, the raw angular displacement and torque data provided by the rheometer were used for analyzing the rheological properties in large amplitude oscillatory shear using the MITlaos program. We recorded Lissajous-Bowditch curves by plotting the instantaneous stress τ (t) against the applied strain γ (t) at a fixed strain amplitude γ_o [34,35].

3. Results and discussion

3.1. Fibroin gelation

Silk fibroin gels are prepared from Bombyx mori cocoons which are composed of sericin and fibroin proteins. The first step toward the gel preparation is to remove sericin proteins from the cocoons and solubilize the resulting fibroin in deionized water. As described in the previous section, the cocoons are first boiled in aqueous Na_2CO_3 solutions to remove sericin and then, the remaining silk fibroin is dissolved in an aqueous solution of concentrated LiBr at 60 °C. After dialyzing against water, an aqueous fibroin solution at a concentration of around 5 w/v% is obtained. Silk fibroin gels are made by mixing this solution with the diepoxide cross-linker BDDE and TEMED catalyst, and then conducting the gelation reactions at 50 °C for 6 h. The concentrations of silk fibroin and BDDE are fixed at 4.2 w/v% and 20 mmol epoxide groups/g silk fibroin, respectively, while the amount of TEMED is varied over a wide range. Fig. 1 represents typical gelation profiles of 4.2 w/v% fibroin solution in the presence of various amounts of TEMED, where the storage modulus G' measured at an angular frequency of 6.3 rad s^{-1} and the loss factor *tan* δ (=G''/G' where G'' is the loss modulus) are shown as a function of the reaction time. TEMED contents together with the pH of the solutions (in parenthesis) are indicated in the figure.

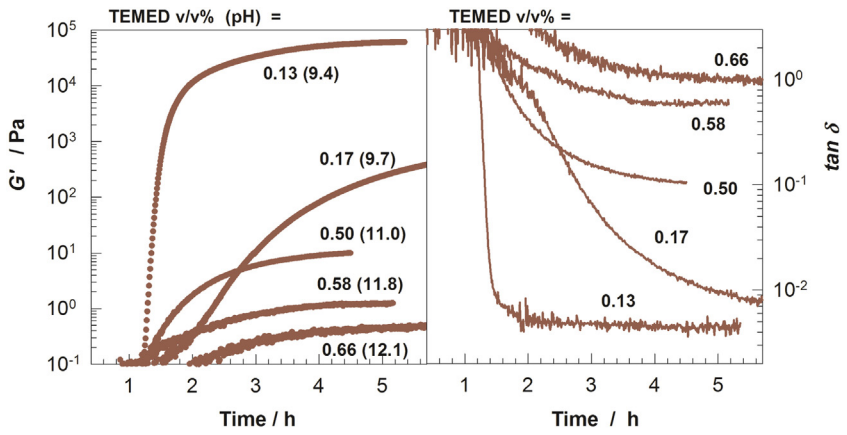

Fig. 1. Storage modulus G', and the loss factor *tan* δ during gelation of aqueous 4.2 w/v% silk fibroin solution at 50 °C. EGDE = 20 mmol/g. TEMED contents and the pHs of the gelation solutions (in parenthesis) are indicated. ω = 6.3 rad s^{-1}. γ_o = 0.01.

In the absence of TEMED, i.e., at pH = 5.7, the storage modulus G' of the fibroin solution does not change over 10 h (not shown in the figure), while in the presence of TEMED, a gel starts to form after an induction period of 60–100 min. A five-orders of magnitude change in G' of fibroin gels could be achieved by varying the TEMED content between 0.1 and 0.7 v/v% corresponding to a range of pH between 9.4 and 12.1. Simultaneously, the loss factor *tan* δ varies between below and above 0.1 indicating formation of strong and weak gels depending on the amount of TEMED. As detailed before [18], the function of TEMED is to adjust the pH of the gelation solution while BDDE attacks the amino groups of fibroin to form interstrand cross-links. Introduction of BDDE-cross-links between the fibroin molecules decreases the mobility of the chains, which triggers the conformational transition in fibroin from random coil to β-sheet structure and hence, fibroin gelation. For instance, fibroin chains before gelation at pH = 5.7 have 12 ± 2% β-sheet structures, while their contribution increases to 55% in the fibroin gels formed between pH = 8–9 [18], which is close to the maximum crystallinity of silk fibroin. As the pH is further increased, this percentage decreases and, at pH = 11, only 20% β-sheets are detected in soluble fibroin chains [18]. Thus, fibroin gels with a storage modulus between 10^{-1}–10^5 Pa and a loss factor between 10^{-2} and 10° could easily be produced within 6 h using this versatile gelation technique.

3.2. Rheological properties and strain stiffening behavior of silk fibroin

The gels formed after a reaction time of 6 h are subjected to stress-relaxation experiments at 25 °C by monitoring the relaxation modulus $G(t, \gamma_o)$ after application of a shear deformation of controlled amplitude γ_o for a duration of 50 s. In Fig. 2, the relaxation modulus $G(t,\gamma_o)$ of fibroin gels prepared at various TEMED concentrations is shown as a function of strain γ_o for times t between 0 and 50 s. In Fig. 3a, all the modulus versus strain data up to the yield strain are collected in a double-logarithmic scale. Several interesting features can be seen from the figures:

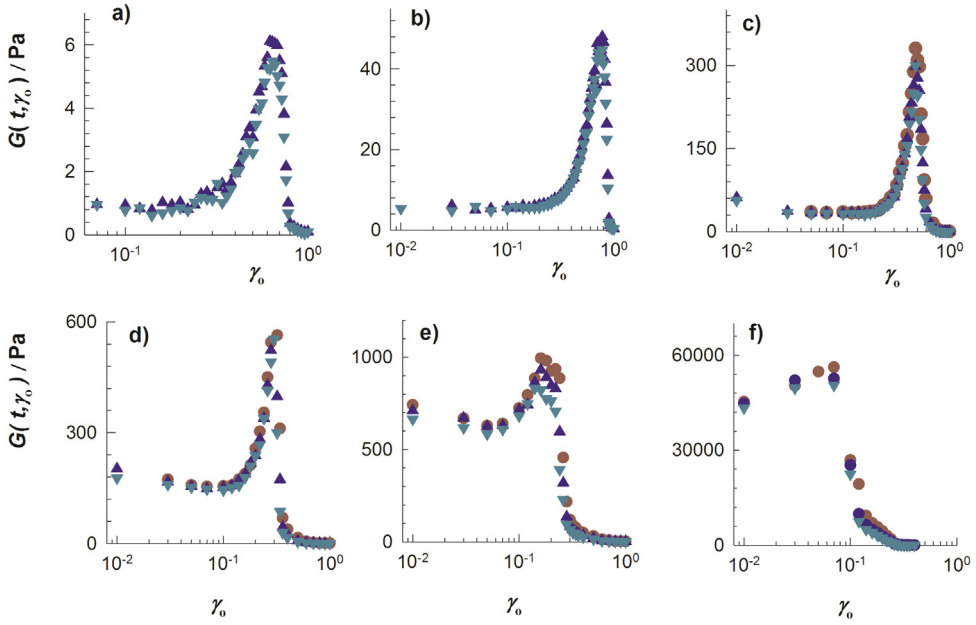

Fig. 2. The relaxation modulus $G(t,\gamma_o)$ of fibroin gels at 25 °C plotted against the strain γ_o for a time scale t = 1 (●), 10 (▲), and 50 s (▼). The amount of TEMED at the gel preparation = 0.66 (a), 0.42 (b), 0.58 (c), 0.25 (d), 0.17 (e), and 0.13% (f).

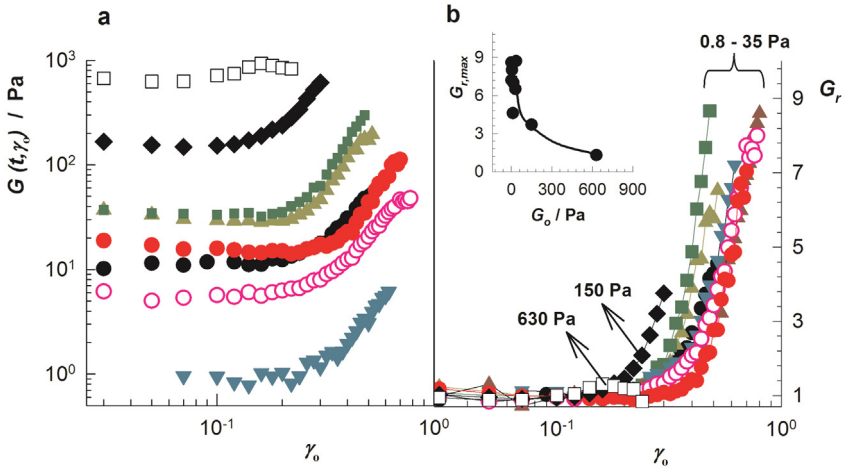

Fig. 3. $G(t,\gamma_o)$ (a) and the reduced modulus G_r (b) of gels formed at various TEMED contents plotted against γ_o. The inset to Fig. 3b shows the extent of stiffening represented by the maximum value of the G_r ($G_{r,max}$) plotted against the linear modulus G_o of fibroin gels. Temperature = 25 °C. For the sake of clarity, only data before the yield strain are plotted. t = 10 s. The linear modulus G_o of some gel samples is indicated in b.

(i) the relaxation modulus $G(t,\gamma_o)$ is independent on the time scale between 0 and 50 s, indicating irreversible nature of cross-links consisting of β-sheet nanostructures,
(ii) $G(t,\gamma_o)$ of the aqueous solution of 4.2 w/v% fibroin remains constant throughout the strain range studied (not shown) while all the fibroin gels derived from this solution exhibit strain stiffening followed by a softening regime beyond the yield point. For gels with a linear modulus between 10^{-1} and 10^{1} Pa, the onset of stiffening appears at a strain of around 0.1 while for the higher modulus gels, the stiffening starts at a lower strain value,
(iii) Except for the gel with the highest linear modulus of around 40 kPa, an initial slight softening appears before the onset of stiffening.

Thus, the general trend of the strain dependence of the modulus $G(t,\gamma_o)$ is the appearance of three regions in the modulus versus strain data, namely an initial slight softening, stiffening, and final softening (rupture) beyond the yield point. Moreover, the most noticeable result shown in Fig. 2 is the appearance of stiffening at a very low strain (10–20% deformation), which is similar to the biological gels consisting of semiflexible filaments [25]. Because silk fibroin is a flexible polymer with a persistence length below 1 nm [36,37], one would expect the onset of stiffening at much larger strain amplitudes. This point will be discussed later in relation with the strain-induced increase in the cross-link density of fibroin gels. In Fig. 3b, the relative increase of the modulus G_r with respect to the linear modulus G_o is plotted against the strain γ_o up to the yield point. Note that the modulus measured in the range of the lowest strain values is denoted as the linear modulus G_o. The inset to the figure shows the extent of stiffening represented by the maximum value of G_r ($G_{r,max}$) plotted against the linear modulus G_o. Up to about 9-fold increase in the modulus could be observed in gels exhibiting a linear modulus between 0.8 and 35 Pa. The extent of stiffening rapidly decreases with increasing G_o indicating that it inversely correlates with the β-sheet content of the gels [18,19]. The lower the β-sheet content, that is, the lower the linear modulus, the stronger is the strain stiffening behavior. The only exception is the aqueous solution of 4.2 w/v% fibroin with the lowest β-sheet content (12 ± 2%) exhibiting no stiffening, which could be attributed to the mobility of flexible fibroin molecules hindering their alignment to form ordered domains.

To understand the internal dynamics of fibroin gels in the stiffening regime, we conduct oscillatory frequency sweep tests at 25 °C

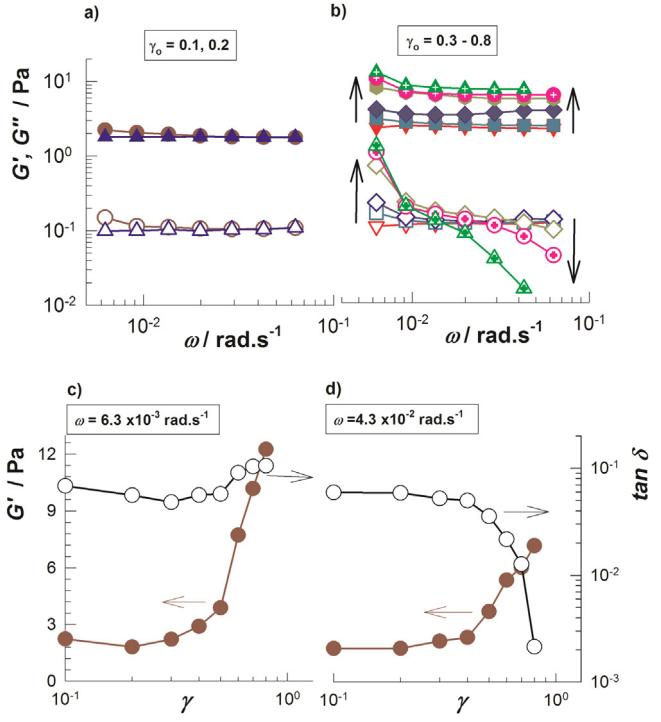

Fig. 4. (a, b): Storage modulus G' (filled symbols) and loss modulus G' (open symbols) of a fibroin gel with a modulus G_o of 2 Pa in the linear (a) and stiffening regimes (b) plotted against the angular frequency ω. The arrows in b indicate the direction of increasing γ_o. Temperature = 25 °C. γ_o = 0.1 (●), 0.2 (▲), 0.3 (▼), 0.4 (■), 0.5 (◆), 0.6 (●), 0.7 (●, x-hair), and 0.8 (▲, x-hair). (c, d): G' (filled symbols) and the loss factor *tan* δ (open symbols) of the same gel plotted against the strain amplitude γ_o. ω = 6.3 × 10^{-3} (c) and 4.3 × 10^{-2} rad.s^{-1}.

over the frequency range 6 × 10^{-3}–6.3 × 10^{-2} rad s^{-1}. The strain amplitude γ_o is fixed at a value between 0.1 and 0.8. The results are collected in Fig. 4a and b for a fibroin gel with a modulus G_o of 2 Pa in the linear and stiffening regimes, respectively, where the storage modulus G' (filled symbols) and the loss modulus G'' (open symbols) are shown as a function of angular frequency ω. The arrows in Fig. 4b indicate the direction of increasing γ_o. In accord with the stress relaxation test results, the storage modulus G' is almost independent on the frequency range studied, corresponding to a time scale between 16 and 170 s. Although the loss modulus G'' is also

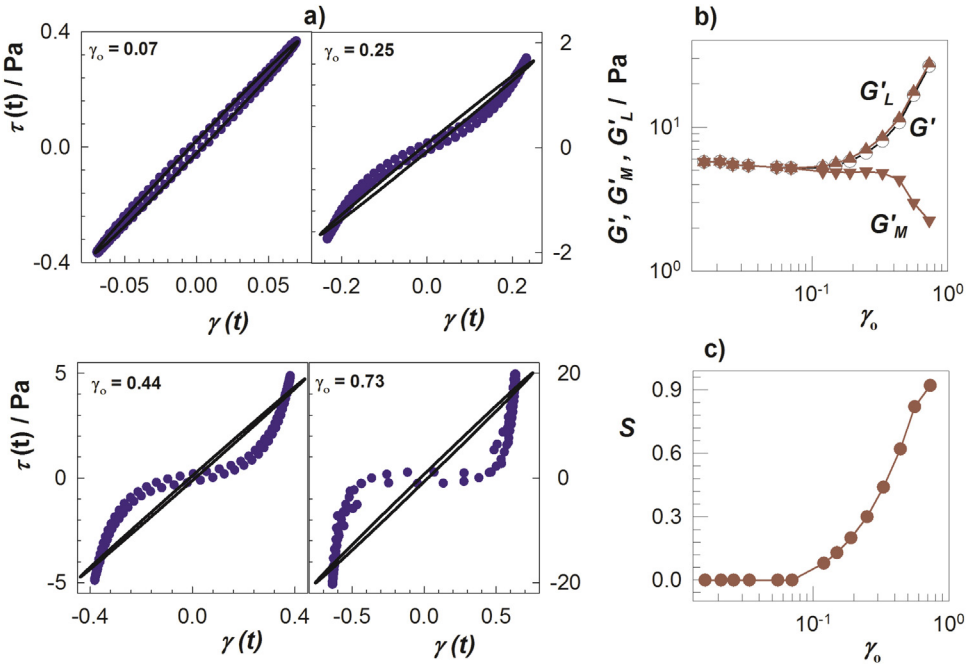

Fig. 5. (a): LB plots for fibroin gel at various strain amplitudes γ_o as indicated. The raw data and the elliptical fits to the data corresponding the first-order harmonic are shown by blue symbols and black curves, respectively. $\omega = 1$ rad s^{-1}. (b,c): The moduli G'_L (▲), G'_M (▼), G' (○), and the non-linearity index S (●) plotted against the strain γ. (For interpretation of the references to colour in this figure legend, the reader is referred to the web version of this article.)

independent on frequency in the linear viscoelastic region (Fig. 4a), it becomes frequency dependent in the stiffening regime (Fig. 4b), and the extent of this dependence increases with increasing strain amplitude γ_o. Fig. 4b also indicates that, at a low frequency, G'' attains a higher value than that in the linear regime indicating viscoelastic energy dissipation at long experimental time scales. In contrast, G'' is smaller at high frequencies indicating that more deformation energy is stored at short times.

The opposite viscoelastic response of strain-stiffened fibroin gels depending on the frequency is also illustrated in Fig. 4c and d, where G' (filled symbols) and the loss factor *tan* δ (open symbols) are plotted against the strain amplitude γ_o at a low and high frequency, respectively. It is seen that the gel during the stiffening regime becomes more viscous or more elastic depending on the time scale of the experiments. At short times (Fig. 4d), the gel is more elastic as compared to its viscoelastic nature in the linear regime while it is more viscous at long times (Fig. 4c). Similar results are also obtained for fibroin gels with various linear modulus G_o (Fig. S1).

We have to mention that the results presented so far are obtained by using the software of the commercial rheometer which assumes a linear rheological response of the gels within each cycle of the oscillatory deformation tests. Thus, it reports the first-harmonic of the elastic response represented by the storage modulus G'. To characterize the nonlinear properties of fibroin gels, we also record Lissajous-Bowditch (LB) curves by plotting the instantaneous stress τ (t) against the applied strain γ (t) at a fixed strain amplitude γ_o [34,35]. Fig. 5a presents typical LB plots of a fibroin gel at a frequency of 1 rad s^{-1} and at four different strain amplitudes γ_o. The raw data of the rheometer and the elliptical fits to the data corresponding the first-order harmonic are shown by blue symbols and black curves, respectively. It is known that LB plots are in a perfect ellipse shape in the linear viscoelastic regime, and the slope of the major axis of the ellipse corresponds to the modulus G'. As seen in Fig. 5a, this behavior is observed at $\gamma_o = 0.07$ at which the gel is in the linear regime. As the strain is increased, LB plots deviate more and more from the elliptical shape indicating nonlinear viscoelastic response of the fibroin gel. As proposed previously [36], the actual elastic response of viscoelastic materials is characterized by the minimum-strain (tangent) modulus G'_M and the large-strain (secant) modulus G'_L. While the tangent modulus G'_M is the slope of the stress-strain plot at zero strain, the secant modulus G'_L is the ratio of stress and strain at maximum strain γ_o, i.e., $G'_M = \left(\partial\tau/\partial\gamma\right)_{\gamma=0}$ and $G'_L = \left(\tau/\gamma\right)_{\gamma=\pm\gamma_0}$. Because the LB plot is elliptical in the linear regime, G'_M and G'_L describing elastic behavior at small and large strains, respectively, converge to the first-harmonic storage modulus G' while the divergency of G'_M from G'_L points out a non-linear response which can be quantified by the index of non-linearity $S = 1 - G'_M/G'_L$. In Fig. 5b and c, the moduli G'_M, G'_L, G', and the non-linearity index S are plotted against the strain γ_o. Initially, all three moduli slightly decrease with increasing γ_o up to 0.07 indicating strain-softening, as observed in Fig. 2. However, although strain-softening requires negative values for the index of non-linearity S, it remains at zero in this range of γ (Fig. 5c), indicating that no instantaneous softening occurs within each oscillatory cycle. At $\gamma_o \geq 0.12$, a difference between G'_M and G'_L appears and S gradually increases with strain implying increasing degree of strain hardening of fibroin network. Moreover, G'_L and G' have similar strain-dependences and they both start to increase at $\gamma_o = 0.12$ while G'_M continues to decrease at large strain values. Similar results were also obtained for fibroin gels with various linear modulus G_o. Thus, the analysis of LB plots leads to the same results as obtained by the first-harmonic of the elastic response and hence, the values of G' and G'' are useful as a framework to discuss the nonlinear viscoelastic properties.

From the above findings, we hypothesize that the non-crystalline domains in silk fibroin re-organize under application of strain into ordered structures acting as additional cross-links and thus contributing to the modulus of gels. The cross-link zones existing in the hardened gels have a transient nature with a lifetime of the order of seconds; at short times, these domains act as strong crosslinks because the loss factor approaches to 10^{-3} (Fig. 4d) while at long times, they dissociate by dissipating energy (Fig. 4c). Thus, if our hypothesis is true, one would expect that the strain stiffen-

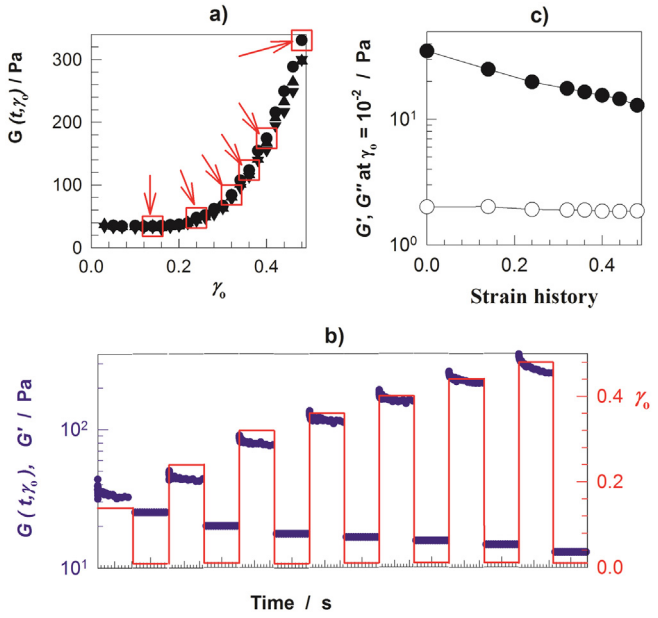

Fig. 6. (a): The relaxation modulus $G(t,\gamma_o)$ of a fibroin gel with a linear modulus of 34 Pa plotted against the strain γ_o for a time scale t = 1 (●), 10 (▲), and 50 s (▼). The square symbols indicated by arrows represent the high strain values γ_{high} selected for six successive stress relaxation and oscillatory time sweep tests. Temperature = 25 °C. (b): The schedule of the stepwise increased strain γ_{high} separated with a low strain γ_{low} (line) and the time dependences of $G(t,\gamma_o)$ at γ_{high} and G' at γ_{low} (blue symbols). (c): The recovered storage G' and loss moduli G'' at γ_{low} plotted against the strain history of the gel. (For interpretation of the references to colour in this figure legend, the reader is referred to the web version of this article.)

ing behavior of fibroin gels is reversible. To understand whether the viscoelastic domains generated in strain-stiffened gels dissociate and re-associate reversibly by on-off switching of the applied strain, we conduct successive stress-relaxation and oscillatory time sweep tests at a high and low strain, respectively. The test consists of the application of a high strain (γ_{high}) and monitoring the relaxation modulus $G(t,\gamma_o)$ of the gel under this strain for a duration of 100 s, followed by immediate reduction of the strain to a low value (γ_{low}), and monitoring the storage G' and loss moduli G'' for 100 s at γ_{low}. In the experiments, γ_{low} is fixed at 0.01 while γ_{high} is stepwise increased from 0.14 to 0.48. The tests are conducted on a fibroin gel with a storage modulus of 34 Pa in the linear regime. Fig. 6a showing the relaxation modulus $G(t,\gamma_o)$ versus strain γ_o plots of this gel at three different time scales reveals 9-fold increase of the modulus with increasing strain up to γ_o = 0.48. The open rectangular symbols in the figure indicated by arrows represent the high strain values γ_{high} selected for six successive stress-relaxation tests. The predetermined schedule of the stepwise increased strain γ_{high} separated by a low strain γ_{low} of 0.01 is shown in Fig. 6b by the red line. The time dependences of the relaxation modulus $G(t,\gamma_o)$ at γ_{high} and the storage modulus G' at γ_{low} are also shown in this figure by the blue symbols. $G(t,\gamma_o)$ immediately increases upon application of the strain γ_{high}, but reversibly, if the strain is reduced to γ_{low}, $G(t,\gamma_o)$ again decreases. The results demonstrate the reversibility of the stiffening behavior of fibroin gel indicating that the associations formed between fibroin molecules due to the applied strain again dissociate under rest. In Fig. 6c, the recovered storage G and loss moduli G'' at γ_{low} are plotted against the strain history of the gel. It is seen that, after removing the high strain γ_{high}, G' decreases below G' of the virgin gel sample while the loss modulus G'' remains unchanged indicating that, although the stiffening in fibroin gel is reversible, its original microstructure is slightly destroyed due to the applied strain.

3.3. Strain stiffening mechanism of silk fibroin

Strain-induced formation of additional cross-links in stiffened gels also explains the appearance of the onset of stiffening at very low strain amplitudes. Otherwise, a significant stiffening in fibroin gels at a very low strain seems unlikely considering the fact that the fibroin molecules isolated from Bombyx mori cocoons by the applied standard method are very flexible polymers with a persistence length below 1 nm [36,37]. For such flexible polymers, the linear viscoelastic regime normally extends to strains above 1 (100% deformation) [25]. In contrast, the biological gels exhibiting such a stiffening behavior consist of semiflexible polymers with a persistence length of a few micrometers which is close to their contour length [25]. As a consequence, the network chains are only slightly coiled between the cross-link zones so that, even at a small deformation, their end-to-end distance approaches their contour length [25,31]. Thus, we can explain significant stiffening in fibroin gels at low strain values with the strain-induced formation of additional cross-links decreasing the contour length of fibroin network chains. In the following paragraphs, we demonstrate that the strain stiffening behavior of fibroin gel can be reproduced by a wormlike chain model taking into account the entropic elasticity of fibroin molecules and the strain induced increase in the cross-link density of fibroin gels. According to the wormlike chain model, an analytical expression for the modulus G can be given by [31,38–40]:

$$G = \frac{1}{2}\,\nu_e\,R\,T\,\nu_2^{0}\left[\frac{4}{3}+\frac{1}{3}\,\frac{(2-z)}{(1-z)^2}\right] \tag{1}$$

where ν_e is the cross-link density of gel, i.e., the number of elastically effective network chains per volume of dry polymer network, ν_2^0 is the volume fraction of cross-linked polymer at the state of gel preparation, R is the gas constant, T is the absolute temperature, and z is the extension ratio of the network chains with respect to its contour length L_c, i.e., $z = r/L_c$, where r is the end-to-end distance of the chain. Assuming that the chains in the 3D fibroin network are isotropically oriented, the extension ratio z is related to the number of segments per network chain N by [31]

$$z = \sqrt{\frac{I_1}{3N}} \tag{2}$$

where I_1 is the state of deformation and equals to $\gamma_o{}^2 + 3$ for simple shear. Moreover, the cross-link density ν_e can also be written in terms of N by

$$\nu_e = (N\,V_r)^{-1} \tag{3}$$

where V_r is the molar volume of a segment. Combining Eqs. (1)–(3), we obtain the following expression for the modulus of gels formed from cross-linked wormlike chains:

$$G = \frac{R\,T\,\nu_2^{0}}{2\,N\,V_r}\left[\frac{4}{3}+\frac{1}{3}\,\frac{\left(2-\sqrt{\frac{\gamma_o{}^2+3}{3N}}\right)}{\left(1-\sqrt{\frac{\gamma_o{}^2+3}{3N}}\right)^2}\right] \tag{4}$$

According to Eq. (4), the modulus G goes to infinity as $\gamma_o \to [3\,(N-1)]^{1/2}$ corresponding to the limit $z \to 1$, i.e., to the full extension of the chain ($r = L_c$). As a consequence, strain stiffening appears at a lower strain as N decreases, that is, as the cross-link density ν_e of the gel increases.

The experimental results already indicate increasing cross-link density of fibroin gels under strain due to the formation of ordered structures acting as additional cross-links. Thus, the number of segments N per network chain is not constant during the rheological tests but it decreases with increasing strain γ_o. Previous works

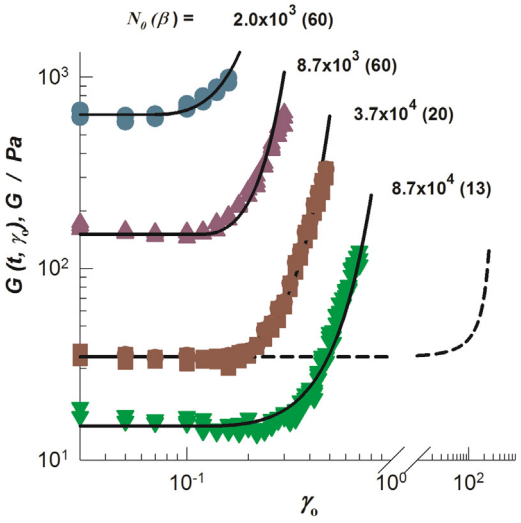

Fig. 7. $G(t,\gamma_o)$ (symbols) and the modulus G calculated using eqs. (4) and (5) (solid curves) of fibroin gels plotted against γ_o. The network chain length N_o and the parameter β (in parenthesis) are shown in the figure. Temperature = 25 °C. TEMED = 0.17 (●), 0.25 (▲), 0.50 (■), and 0.58 v/v% (▼). The dashed curve represents the theoretical G versus γ_o dependence for the gel formed at 0.50 v/v% TEMED for the condition $N = N_o$.

reveal that the increase of the moduli of most biopolymer gels due to the applied strain can be represented by the simple relation [41], $G/G_o = \exp\left(\gamma_o/\gamma^*\right)^2$, where γ^* is a fitting parameter representing the critical value of γ_o above which strain stiffening effect dominates the network behavior. Here, we also use a similar exponential relation to describe the decrease of the network chain length N due to the applied strain:

$$N = N_o \exp\left[-\beta(\gamma_o - \gamma_a)^2\right] \quad (5)$$

where γ_a is the critical strain at the onset of hardening and β is a parameter relating to the rate of the cross-link density increase with strain. Thus, the gel is in the linear regime as long as $\gamma_o \leq \gamma_a$ while strain hardening appears at larger strains. On the other hand, the term in the square bracket in Eq. (4) goes to 2 in the limit $\gamma_o \to 0$, so that the equation reduces to

$$G_o = \frac{RT\nu_2^0}{N_o V_r} \quad (6)$$

which is the expression for the modulus G_o of the gel in the linear regime. To predict the strain stiffening behavior of fibroin gels, we evaluate the parameters in Eqs. (4)–(6) as follows: We first calculate the average molar volume of the repeat unit of silk fibroin from its composition as 70 mL mol^{-1}, which is taken as the molar volume V_r of a segment. The volume fraction ν_2^0 of fibroin at the state of gel preparation is calculated from the fibroin concentration (4.2 w/v%) and the density of fibroin (1.35 g mL^{-1} [42]) as 0.031. Using these parameters together with the linear modulus G_o of fibroin gels, we solve Eq. (6) for the number of segments N_o per fibroin network chain in the linear regime. Then, Eqs. (4) and (5) are solved for the parameter β in order to reproduce the experimental modulus versus strain data.

In Fig. 7, the symbols represent the modulus $G(t,\gamma_o)$ data of fibroin gels as a function of strain γ_o while the solid curves are best fit curves using Eqs. (4) and (5). The values of the parameter β estimated from the fits together with the initial number of segments N_o per network chain are also shown in the figure. Let us first consider the data of the fibroin gel with a network chain length N_o of 3.7×10^4 (square symbols). Assuming that N_o remains constant under application of strain (β = 0), Eq. (4) predict the onset of stiffening at a strain γ_o of around 40 (4000% deformation), as indicated by the dashed curve in Fig. 6. The solid curve is the best fitting curve to the experimental data of this gel and yields β = 20. Fig. 6 shows that the experimental data can well be reproduced by the wormlike chain model taking into account the entropic elasticity of fibroin molecules and the increase of the cross-link density of fibroin gels under application of strain. The parameter β of the model increases with decreasing chain length N_o, that is with increasing linear modulus G_o of fibroin gels. This is reasonable because decreasing network chain length will increase the probability of intermolecular hydrogen bonding and hydrophobic interactions so that the rate of formation of additional cross-links and hence, the magnitude of β increases. We have to note that no good fit to the experimental data could be obtained at a linear modulus below 10 Pa (Fig. S2), which we attribute to the network imperfections leading to a deviation from the rubber elasticity assumptions.

4. Conclusions

The linear and nonlinear viscoelastic properties as well as the reversibility of strain stiffening behavior of silk fibroin gels are investigated by rheological measurements. We prepare fibroin gels from 4.2 w/v% fibroin solution in the presence of BDDE and TEMED as a cross-linker and catalyst, respectively. By changing TEMED concentration in the gelation system, we were able to obtain fibroin gels with a storage modulus G' between 10^{-1}–10^5 Pa and a loss factor $tan\ \delta$ between 10^{-2} and 10°. We observe a strong stiffening in fibroin gels with increasing strain above 10% deformation. Up to about 9-fold increase in the modulus could be observed in fibroin gels exhibiting a linear modulus between 0.8 and 35 Pa. The extent of stiffening rapidly decreases with increasing linear modulus G_o indicating that it inversely correlates with the β-sheet content of fibroin gels. The strain stiffening behavior of fibroin gels is reversible, that is, if the strain is removed, the stiffened gel recovers its initial viscoelastic properties. We also show that the strain induced formation of transient intermolecular domains acting as reversible cross-links are responsible for the stiffening behavior of fibroin gels. These additional cross-links formed in hardened fibroin gels have a temporary nature with lifetimes of the order of seconds. The nonlinear behavior of fibroin gels can be reproduced by a wormlike chain model taking into account the entropic elasticity of fibroin molecules and the strain induced increase in the cross-link density of fibroin gels.

Acknowledgments

This work was supported by the Scientific and Technical Research Council of Turkey (TUBITAK), KBAG 114Z312. OO thanks the Turkish Academy of Sciences (TUBA) for the partial support.

Appendix A. Supplementary data

Supplementary data associated with this article can be found, in the online version, at http://dx.doi.org/10.1016/j.ijbiomac.2016.11.034.

References

[1] C. Vepari, D.L. Kaplan, Silk as a biomaterial, Prog. Polym. Sci. 32 (2007) 991–1007.
[2] F. Vollrath, D. Porter, Silks as ancient models for modern polymers, Polymer 50 (2009) 5623–5632.
[3] J.G. Hardy, L.M. Romer, T.R. Scheibel, Polymeric materials based on silk proteins, Polymer 49 (2008) 4309–4327.
[4] C.Z. Zhou, F. Confalonieri, N. Medina, Y. Zivanovic, C. Esnault, T. Yang, M. Jacquet, J. Janin, M. Duguet, R. Perasso, Z.G. Li, Fine organization of Bombyx mori fibroin heavy chain gene, Nucleic Acids Res. 28 (2000) 2413–2419.
[5] H.J. Jin, D.L. Kaplan, Mechanism of silk processing in insects and spiders, Nature 424 (2003) 1057–1061.

[6] U.J. Kim, J. Park, C. Li, H.J. Jin, R. Valluzzi, D.L. Kaplan, Structure and properties of silk hydrogels, Biomacromolecules 5 (2004) 786–792.
[7] A. Matsumoto, J. Chen, A.L. Collette, U.J. Kim, G.H. Altman, P. Cebe, D.L. Kaplan, Mechanisms of silk fibroin sol-gel transitions, J. Phys. Chem. B 110 (2006) 21630–21638.
[8] J. Magoshi, Y. Magoshi, S. Nakamura, Mechanism of fiber formation of silkworm, in: D. Kaplan, W.W. Adams, B. Farmer, C. Viney (Eds.), Silk Polymers, American Chemical Society, Washington, 1994, pp. 292–310.
[9] A. Matsumoto, A. Lindsay, B. Abedian, D.L. Kaplan, Silk fibroin solution properties related to assembly and structure, Macromol. Biosci. 8 (2008) 1006–1018.
[10] X. Chen, D.P. Knight, F. Vollrath, Rheological characterization of Nephila spidroin solution, Biomacromolecules 3 (2002) 644–648.
[11] A.E. Terry, D.P. Knight, D. Porter, F. Vollrath, pH induced changes in the rheology of silk fibroin solution from the middle division of Bombyx mori silkworm, Biomacromolecules 5 (2004) 768–772.
[12] C. Dicko, F. Vollrath, J.M. Kenney, Spider silk protein refolding is controlled by changing pH, Biomacromolecules 5 (2004) 704–710.
[13] X.H. Zong, P. Zhou, Z.Z. Shao, S.M. Chen, X. Chen, B.W. Hu, F. Deng, W.H. Yao, Effect of pH and copper(II) on the conformation transitions of silk fibroin based on EPR NMR, and Raman spectroscopy, Biochemistry 43 (2004) 11932–11941.
[14] C. Dicko, J.M. Kenney, D. Knight, F. Vollrath, Transition to a beta-sheet-rich structure in spidroin in vitro: the effects of pH and cations, Biochemistry 43 (2004) 14080–14087.
[15] A. Ochi, K.S. Hossain, J. Magoshi, N. Nemoto, Rheology and dynamic light scattering of silk fibroin solution extracted from the middle division of Bombyx mori silkworm, Biomacromolecules 3 (2002) 1187–1196.
[16] K.S. Hossain, A. Ochi, J. Magoshi, N. Nemoto, Dynamic light scattering of native silk fibroin solution extracted from different parts of the middle division of the silk gland of the Bombyx mori silkworm, Biomacromolecules 4 (2003) 350–359.
[17] X. Chen, D.P. Knight, Z.Z. Shao, F. Vollrath, Conformation transition in silk protein films monitored by time-resolved Fourier transform infrared spectroscopy: effect of potassium ions on Nephila spidroin films, Biochemistry 41 (2002) 14944–14950.
[18] I. Karakutuk, F. Ak, O. Okay, Diepoxide-triggered conformational transition of silk fibroin: formation of hydrogels, Biomacromolecules 13 (2012) 1122–1128.
[19] F. Ak, Z. Oztoprak, I. Karakutuk, O. Okay, Macroporous silk fibroin cryogels, Biomacromolecules 14 (2013) 719–727.
[20] T. Yucel, P. Cebe, D.L. Kaplan, Vortex-induced injectable silk fibroin hydrogels, Biophys. J. 97 (2009) 2044–2050.
[21] E. Servoli, D. Maniglio, A. Motta, C. Migliaresi, Folding and assembly of fibroin driven by an AC electric field: effects on film properties, Macromol. Biosci. 8 (2008) 827–835.
[22] G.G. Leisk, T.J. Lo, T. Yucel, Q. Lu, D.L. Kaplan, Electrogelation for protein adhesives, Adv. Mater. 22 (2010) 711–715.
[23] T. Yucel, N. Kojic, G.G. Leisk, T.J. Lo, D.L. Kaplan, Non-equilibrium silk fibroin adhesives, J. Struct. Biol. 170 (2010) 406–412.
[24] A.P. Tabatabai, D.L. Kaplan, D.L. Blair, Rheology of reconstituted silk fibroin protein gels: the epitome of extreme mechanics, Soft Matter 11 (2015) 756–761.
[25] C. Storm, J.J. Pastore, F.C. MacKintosh, T.C. Lubensky, P.A. Janmey, Nonlinear elasticity in biological gels, Nature 435 (2005) 191–194.
[26] J. Xu, Y. Tseng, D. Wirtz, Strain hardening of actin filament networks, J. Biol. Chem. 275 (2000) 35886–35892.
[27] M.L. Gardel, J.H. Shin, F.C. MacKintosh, L. Mahadevan, P. Matsudaira, D.A. Weitz, Elastic behavior of cross-linked and bundled actin networks, Science 304 (2004) 1301–1305.
[28] M.L. Gardel, K.E. Kasza, C.P. Brangwynne, J. Liu, D.A. Weitz, Mechanical response of cytoskeletal networks, Methods Cell Biol. 89 (2008) 487–519.
[29] J.V. Shah, P.A. Janmey, Strain hardening of fibrin gels and plasma clots, Rheol. Acta 36 (1997) 262–268.
[30] N.A. Kurniawan, L.H. Wong, R. Rajagopalan, Early stiffening and softening of collagen: interplay of deformation mechanisms in biopolymer networks, Biomacromolecules 13 (2012) 691–698.
[31] N. Orakdogen, B. Erman, O. Okay, Evidence of strain hardening in DNA gels, Macromolecules 43 (2010) 1530–1538.
[32] S. Abdurrahmanoglu, M. Cilingir, O. Okay, Dodecyl methacrylate as a crosslinker in the preparation of tough polyacrylamide hydrogels, Polymer 52 (2011) 694–699.
[33] K.C. Tam, R.D. Jenkins, M.A. Winnik, D.R. Bassett, A structural model of hydrophobically modified urethane-ethoxylate (HEUR) associative polymers in shear flows, Macromolecules 31 (1998) 4149–4159.
[34] R.H. Ewoldt, A.E. Hosoi1, G.H. McKinley, New measures for characterizing nonlinear viscoelasticity in large amplitude oscillatory shear, J. Rheol. 52 (2008) 1427–1458.
[35] K. Hyun, M. Wilhelm, C.O. Klein, K.S. Cho, J.G. Nam, K.H. Ahn, S.J. Leed, R.H. Ewoldt, G.H. McKinley, A review of nonlinear oscillatory shear tests: analysis and application of large amplitude oscillatory shear (LAOS), Prog. Polym. Sci. 36 (2011) 1697–1753.
[36] H. Shulha, C.W.P. Foo, D.L. Kaplan, V.V. Tsukruk, Unfolding the multi-length scale domain structure of silk fibroin protein, Polymer 47 (2006) 5821–5830.
[37] B.P. Partlow, A.P. Tabatabai, G.G. Leisk, P. Cebe, D.L. Blair, D.L. Kaplan, Silk fibroin degradation related to rheological and mechanical properties, Macromol. Biosci. 16 (2016) 666–675.
[38] R.W. Ogden, G. Saccomandi, I. Sgura, On worm-like chain models within the three-dimensional continuum mechanics framework, Proc. R. Soc. A 462 (2006) 749–768.
[39] J.F. Marko, E.D. Siggia, Stretching DNA, Macromolecules 28 (1995) 8759–8770.
[40] J.E. Mark, B. Erman, Rubberlike Elasticity. A. Molecular Primer, Cambridge University Press, New York, 2007.
[41] K.A. Erk, K.J. Henderson, K.R. Shull, Strain stiffening in synthetic and biopolymer networks, Biomacromolecules 11 (2010) 1358–1363.
[42] S.J. Park, K.Y. Lee, W.S. Ha, S.Y. Park, Structural changes and their effect on mechanical properties of silk fibroin/chitosan blends, J. Appl. Polym. Sci. 74 (1999) 2571–2575.